Shape memory behavior of biocompatible polyurethane stereoelastomers synthesized via thiol-yne Michael addition

Hsu, Yen-Hao; Luong, Derek; Asheghali, Darya; Dove, Andrew; Becker, Matthew L

DOI:
10.1021/acs.biomac.1c01473

Document Version
Peer reviewed version

Citation for published version (Harvard):
Hsu, Y-H, Luong, D, Asheghali, D, Dove, A & Becker, ML 2022, 'Shape memory behavior of biocompatible polyurethane stereoelastomers synthesized via thiol-yne Michael addition', *Biomacromolecules*, vol. 23, no. 3, pp. 1205-1213. https://doi.org/10.1021/acs.biomac.1c01473

Shape Memory Behavior of Biocompatible Polyurethane StereoElastomers Synthesized *via* Thiol-yne Michael Addition

Yen-Hao Hsu,[a] Derek Luong,[a] Darya Asheghali,[a] Andrew P. Dove,*[b] Matthew L. Becker*[a, c]

[a] Department of Chemistry, Duke University, Durham, NC, 27708, United States

[b] School of Chemistry, University of Birmingham, Birmingham B15 2TT, United Kingdom

[c] Departments of Mechanical Engineering and Materials Science, Biomedical Engineering, Orthopaedic Surgery Duke University, Durham, NC, 27708, United States

KEYWORDS: Thiol-yne, Michael addition, urethane, hydrogen bonding, shape memory, elastomer

ABSTRACT: Biodegradable shape memory elastomers have the potential for use in soft tissue engineering, drug delivery and device fabrication applications. Unfortunately, few materials are able to meet the targeted degradation and mechanical properties needed for long-term implantable devices. In order to overcome these limitations, we have designed and synthesized a series of unsaturated polyurethanes that are elastic, degradable and non-toxic to cells *in vitro*. The polymerization included a nucleophilic thiol-yne Michael addition between a urethane-based dipropiolate and a dithiol to yield an *α,β*-unsaturated carbonyl moiety along the polymer backbone. The alkene stereochemistry of materials was tuned between 32-82% *cis* content using the combination of an organic base and solvent polarity which collectively direct the nucleophilic addition. The bulk properties such as tensile strength, modulus, and glass transition temperature can also be tuned broadly, and the hydrogen bonding imparted by the urethane moiety allows for these materials to elicit cyclic shape memory behavior. We also demonstrated the *in vitro* degradation properties are highly dependent on the alkene stereochemistry.

INTRODUCTION

Polyurethanes (PUs)[1, 2] are used widely in commercial products such as foams,[3-5] coatings,[2, 6, 7] adhesives,[2, 8] and medical devices[9-12] due to their unique and tunable thermoplastic and thermoset properties. Polyurethanes are also used in biomedical applications including short-term implants such as surgical sutures,[13, 14] catheters,[12, 15-17] and wound dressings.[18-20] Polyurethanes have also been used in shape memory applications.[9, 21, 22] This behavior arises from interactions among the hydrogen bonding networks that arise between the urethane groups.

Shape memory polymers (SMPs) are materials that can be deformed to a temporary shape that is 'locked in' until an external stimulus is applied (i.e. electromagnetic field,[23] light,[24] and heat[25]) which allows the material to return to the original shape. Several clever synthetic and architectural strategies have utilized shape memory triggered by pH changes for drug delivery[26] while others have used temperature for stent deployment following placement *in vivo*.[27] For materials seeking use thermally induced shape memory for biomedical applications, the source of thermally stimulated shape memory recovery should ideally come from the physiological temperature of the human body (~ 37 °C). For this reason, thermally-induced SMPs have been widely studied.[21, 28]

Thermal and mechanical properties of most well-known polyurethanes (PUs) can be modified by changing the hard segments (usually arising from diisocyanate derivatives), soft segments (from diols), and chain extenders (from oligomeric diols or ester diols).[29] The wide-ranging types of hydrolytically degradable segments including esters, anhydrides have been incorporated widely as well.[30] The conventional step growth polymerization method utilized for polyurethanes includes the use of a diisocyanate and a diol with a tin catalyst in an anhydrous system. Unfortunately, unstable carbamic acid could be formed from unremoved water with isocyanate, then rapidly decomposes into carbon dioxide and an amine, which can react with additional isocyanate to afford a urea linkage that could cause undesired properties from uncontrolled and unrepeatable molecular mass distribution.[1] Accordingly, the search for a simple and tolerant method to produce polyurethanes (PUs) with biodegradable, and/or resorbable units for long-term implant has been of interest for the materials science community.

Altering stereochemistry in nature has evolved into a way to control mechanical properties (i.e., natural rubber and gutta-percha).[31, 32] Property differences among these materials are due to the stereochemistry[33] (cis vs. trans) of the alkene moiety within the polymer backbone and the elastic properties from natural rubber in particular arise

from its high *cis* content which enhances the interchain packing. Stereo-chemically controlled addition within synthetic polymers has recently been accomplished by nucleophilic thiol-yne Michael addition yielding *α,β*-unsaturated carbonyl moieties along the polymer backbone.[28, 34-36] These materials have been found to have tunable thermal and mechanical properties which are highly desirable. Regarded as an efficient synthetic tool, the *cis*/*trans* ratio can be altered by choices of or organic base catalyst and solvent polarity without changing the stoichiometric composition of the final polymer materials. Additionally, the polymerization is easily scalable without an anhydrous reaction environment.[35, 36]

Herein, we strategically designed and synthesized a urethane-based dipropiolate, 5,14-dioxo-4,15-dioxa-6,13-diazaoctadecane-1,18-diyl dipropiolate, as a novel monomer made from bromo-substituted carbamate and further nucleophilic substitution. The subsequent polymerization can be achieved by utilizing the efficient thiol-yne Michael reaction between the urethane-based dipropiolate and distilled 1,6-hexanedithiol to yield an unsaturated polyurethane. The control over stereochemistry of *α, β*-unsaturated carbonyl moiety along the backbone provides tunable thermal and mechanical properties of which we showcased by exploiting different solvents (DMSO and/or $CHCl_3$) and amine catalysts (Et_3N or DBU) to achieve various configuration of *cis* double bond content. The urethane unit of the polymer chain displayed high potential shape memory behavior based on hydrogen bonding networks. Moreover, the hydrogen bonding interaction of thiol-yne polyurethanes was found to enhance mechanical properties with relatively low *cis* content. Significantly, polymers with various *cis* content were all found to be amorphous and *in vitro* investigation including accelerated degradation and cell viability indicated excellent biostability and biocompatibility.

EXPERIMENTAL SECTION

Materials. All reagents and solvents were used as received without further purification except 1,6-hexanedithiol. The chloroform-*d* ($CDCl_3$) and was purchased from Cambridge Isotopes Laboratories, Inc (Tewksbury, MA). Chloroform was purchased from VWR (Raleigh, NC; ACS Grade, stabilized with amylene). Diethyl ether (Et_2O) and isopropyl alcohol (^{i}PrOH) were purchased from EMD Millipore (Burlington, MA). Anhydrous methylene chloride (CH_2Cl_2), ethyl acetate (EtOAc), *N*,*N*-dimethylformamide (DMF), dimethyl

sulfoxide (DMSO), methanol (MeOH), sodium hydroxide (NaOH), sodium sulfate (Na_2SO_4), sodium bicarbonate ($NaHCO_3$), ammonium chloride (NH_4Cl), propiolic acid, 3-bromo-1-propanol, hexamethylene diisocyanate (HDI), dibutyltin dilaurate, 1,8-diazabicyclo[5.4.0]undec-7-ene (DBU), triethylamine (Et_3N), hexanes, butylated hydroxytoluene (BHT), were purchased from Sigma-Aldrich (Milwaukee, WI).

Characterization. ^1H and ^{13}C NMR spectra were obtained using a Varian Mercury 300 MHz NMR spectrometer operated at 303 K. All chemical shifts are reported in ppm (δ) and referenced to the chemical shifts of residual solvent resonances ($CDCl_3$ ^1H: δ = 7.26 ppm, ^{13}C: δ = 77.16 ppm).

Differential scanning calorimetry (DSC) was performed using a TA Instruments Q200 DSC (TA Instruments – Waters L.L.C., New Castle, DE) on sample sizes between 5 – 10 mg using temperature heating ramps of 10 °C·min^{-1} and a cooling rate of 10 °C·min^{-1} from -30 °C to 150 °C. The glass transition temperature (T_g) was determined from the midpoint in the second heating cycle of DSC. The crystalline temperature (T_c) and the melting temperature (T_m) were obtained at 1 °C·min^{-1} in the second heating cycle.

Thermogravimetric analysis (TGA) was performed using a TA Instruments TGA Q50 (TA Instruments – Waters L.L.C, New Castle, DE) on sample sizes of ca. 10 mg using a heating ramp of 20 °C·min^{-1} from r.t. to 800 °C. The decomposition temperature (T_d) was determined at 5% weight loss.

Size exclusion chromatography (SEC) was performed on all samples using an EcoSEC HLC-8320 GPC (Tosoh Bioscience LLC, King of Prussia, PA) equipped with a TSKgel GMH_{HR}-M mixed bed column and refractive index (RI) detector. Molecular masses were calculated using a calibration curve determined from polystyrene standards (PStQuick MP-M standards, Tosoh Bioscience, LLC) with DMF with 0.1 M LiBr as eluent flowing at 1.0 mL·min^{-1} at 323K, and a sample concentration of 3 mg·mL^{-1} from DMF/ DMSO (v/ v 1:1).

Infrared (IR) spectra of 0.5 mm 82% *cis* polymer thin films (before and after stretched) were collected on a Nicolet i550 FT-IR (Thermo Scientific) (32 scans, 8 cm^{-1} resolution).

Mechanical Property Measurements. *Tensile Tests at Different Strain Rates:* Thin films of each polymer

were fabricated using a vacuum compression machine (TMP Technical Machine Products Corp.). The machine was preheated to 150 °C. Polymer was then added into the 50 × 50 × 0.5 mm mold and put into the compression machine with vacuum on. After 15 minutes of melting, 5 lbs*1000, 10 lbs*1000, 20 lbs*1000 of pressure were applied for 5 minutes, respectively. Following compression, the mold was cooled while maintaining 20 lbs*1000 of pressure to prevent wrinkle formation on the film's surface. The films were visually inspected to ensure that no bubbles were present. Dumbbell-shaped samples were cut using a custom ASTM Die D-638 Type V. Strain rates of 0.1, 1, 5, 10, 20 mm/min were used and a rate of 10 mm/min was determined to be appropriate. Tensile tests at different stretching velocities were carried out using an Instron 5567 Universal Testing Machine at 25 °C. The gauge length was set as 7 mm and the neck dimensions of the specimens were 7.11 mm in length, 1.70 mm in width and 0.50 mm in thickness.

Tensile Tests at 10 mm/min: Dumbbell-shaped samples were prepared using the same method as noted above. Tensile tests were carried out using Instron 5567 Universal Testing Machine at 25 °C. The gauge length was set as 7 mm and the crosshead speed was set as 10 mm/min. The dimensions of the neck of the specimens were 7.11 mm in length, 1.70 mm in width and 0.50 mm in thickness. Modulus was obtained from the slope of the initial linear region. The reported results are average values from three individual measurements.

Dynamic Mechanical Analysis (DMA). *Temperature Sweep Data:* Rectangular DMA specimens (25 x 5 x 0.5 mm) were prepared by compression molding. Single frequency (1 Hz), strain-based (15 μm amplitude), temperature sweep (-50 to 120 ºC at a rate of 3 °C·min^{-1}) experiments were conducted on three independent samples.

Shape Memory Characterization: Cyclic thermomechanical testing was conducted using a DMA Q800 instrument. Testing was completed in controlled force mode with heating and cooling rates of 10 °C·min^{-1}. The fixity and recovery parameters for shape memory were calculated using the standard shape memory equations shown in previous literature.[37]

***In Vitro* Accelerated Degradation.** A film in 0.5 mm thickness of each elastomer was prepared from vacuum

compression mold using the same method as stated above. Discs with 4 mm in diameter were cut from the film and placed in 5 M NaOH solution in the incubator (37 ºC + 5% CO_2 humidified atmosphere) for up to 12 weeks. The films absorbed, degraded, swelled and the 5 M NaOH solution was changed every week to ensure the degradation process. At specified intervals (1^{st}, 2^{nd}, 4^{th}, 8^{th}, and 12^{th} week respectively), the samples were removed, dried and weighed. The results of mass changes are the average values of four individual samples for each material at each time point. The surface changes during degradation were characterized using field emission scanning electron microscopy (SEM, JSM-7401F, JEOL, Peabody, MA).

Cell Viability Studies. *Cell seeding onto polymer thin films:* Mouse fibroblast cells (L929, passage 8) were cultured using Eagle's Minimum Essential Medium (ATCC) supplied with 10 vol. % horse serum, 100 units/mL penicillin, and 100 µg/mL streptomycin at 37 °C + 5% CO_2. Cells were subcultured every 3 days with 0.25% (w/v) trypsin and 0.5% (w/v) EDTA solution. Films were sterilized by ethylene oxide (EtO) using an Anprolene AN74i sterilizer (Andersen Products) for 12 h followed by a purge cycle for 48 h. Samples were washed 3× with PBS prior to cell seeding. Cells were seeded on the polymer thin films at 30,000 cells/cm^2. For positive and negative controls, cells were seeded on glass slides.

LIVE/DEAD imaging of cells seeded on polymer thin films: 48 h after cell seeding, polymer thin film and positive control glass slides were washed 3× with PBS and soaked in a LIVE/DEAD solution (Molecular Probes, Invitrogen) containing 5 µL of 4 mM calcein AM and 5 µL of 2 mM ethidium homodimer-1 in 5 mL PBS for 30 minutes. Samples were then mounted with mounting media and imaged at 20× magnification using a Keyence BZ-X700 microscope with filters for Texas Red and GFP. For the negative control, cells on glass slides were soaked in 70% EtOH for 1 h prior to staining, then processed identically to the experimental and positive control groups.

Cell viability as measured by XTT: The XTT (2,3-bis-(2-methoxy-4-nitro-5-sulfophenyl)-2H-tetrazolium-5-carboxanilide) assay (Biotium) was used to measure cell viability. For the experimental and positive controls, 48 h after seeding, growth media was replaced with 300 µL fresh media. For negative controls, growth media was replaced with 70% EtOH for 1 h, followed by replacing the 70% EtOH with 300 µL fresh media. Next, 75 µL of

XTT solution was added and the sample was then incubated for 4 h at 37 °C + 5% CO_2. Following incubation, the absorbance at 500 nm (A_{500}) of the growth media solution was measured. Percent viability of the cells seeded on the polymer sample was calculated by the equation below,

$$Viability = \frac{A_{500}(Exp) - A_{500}(Neg)}{A_{500}(Pos) - A_{500}(Neg)} \times 100$$

where "Exp", "PC", and "NC" refer to the experimental, positive control, and negative control groups respectively.

Syntheses of Monomer and Polymers. *Bis(3-bromopropyl) hexane-1,6-diyldicarbamate (2):* Under anhydrous condition, hexamethylene diisocyanate (24.00 mL, 0.15 mol), 3-bromo-1-propanol (30.00 mL, 0.33 mol) were dissolved in anhydrous DCM (200 mL) and the mixture was cooled to 0 °C for 10 min before a drop of dibutyltin dilaurate as catalyst was added in one aliquot. The reaction was kept at 0 °C for additional 10 min then warmed to room temperature and stirred overnight. The reaction solution was precipitated in diethyl ether (500 mL), filtered, washed again by additional diethyl ether (500 mL), and collected. The collected precipitate was dried by high vacuum system at room temperature for 24 h to obtain the product as a white powder (52.00 g, 78%). ^{1}H NMR (300 MHz, $CDCl_3$) δ 4.69 (br, 2H), 4.19 (t, J = 6 Hz, 4H), 3.46 (t, J = 6 Hz, 4H), 3.16 (q, J = 6 Hz, 4H), 2.16 (quint, J = 6 Hz, 4H), 1.54-1.45 (m , 4H), 1.36-1.30 (m, 4H). ^{13}C NMR (75 MHz, $CDCl_3$) δ 156.47, 62.53, 40.88, 32.29, 29.95, 29.74, 26.30. ESI-MS for $C_{14}H_{26}Br_2N_2O_4Na$, m/z theoretical: $[M+Na]^+$ = 469.01 Da, observed: $[M+Na]^+$ = 469.0 Da.

5,14-Dioxo-4,15-dioxa-6,13-diazaoctadecane-1,18-diyl dipropiolate (U_6): In the dark hood, bis(3-bromopropyl) hexane-1,6-diyldicarbamate (2) (10.00 g, 0.022 mol) and sodium propiolate[38] (5.15 g, 0.056 mol) were dissolved in DMF (150 mL), then the mixture was heated up to 50 °C, and stirred for 24 h. After the reaction was cooled to room temperature, a saturated solution of NH_4Cl (200 mL) was added to the mixture and stirred for 10 min. The mixture was extracted with ethyl acetate (150 mL × 3) and the organic extracts were combined. The extracted organic solution was extracted further with a saturated solution of $NaHCO_3$ (150 mL× 3) to remove excess acid. The organic layer was combined and dried over anhydrous Na_2SO_4, filtered, and concentrated. The residue was purified by flash column chromatography on silica gel (EtOAc/ hexanes 2:1; R_f = 0.35) twice. After removal

of the solvent, the final product was dried under high vacuum to yield the product as a white powder (6.66 g, 70%). ^{1}H NMR (300 MHz, $CDCl_3$) δ 4.74 (br, 2H), 4.27 (t, J = 6 Hz, 4H), 4.14 (t, J = 6 Hz, 4H), 3.15 (q, J = 6 Hz, 4H), 3.12 (s, 2H), 1,99 (quint, J = 6 Hz, 4H), 1.51-1.47 (m, 4H), 1.35-1.32 (m, 4H). ^{13}C NMR (75 MHz, $CDCl_3$) δ 156.46, 152.77, 75.05, 74.67, 63.15, 61.05, 40.89, 29.96, 28.17, 26.63. ESI-MS for $C_{20}H_{28}N_2O_8Na$, m/z theoretical: $[M+Na]^+$ = 447.17 Da, observed: $[M+Na]^+$ = 447.1 Da.

General procedure of thiol-yne step-growth polymerization for polymer U_6T_6: Synthesis of 82% *cis* content was taken as example. 5,14-Dioxo-4,15-dioxa-6,13-diazaoctadecane-1,18-diyl dipropiolate (U_6, 2.82 g, 6.6×10^{-3} mol) and 1,6-hexanedithiol (T_6, 1.00 g, 6.6×10^{-3} mol) were added to a 100 mL round bottom flask with 20 mL $CHCl_3$. The solution was then cooled to -15 °C with stirring for 15 min before 1,8-diazabicyclo[5.4.0]undec-7-ene (10 μL, 6.6×10^{-5} mol) was added in one aliquot. Notably, the addition of DBU caused the solution to boil due to an exothermic reaction. After 10 min, the reaction was allowed to warm to room temperature. After 1 h, excess of 5,14-dioxo-4,15-dioxa-6,13-diazaoctadecane-1,18-diyl dipropiolate was dissolved in 5 mL $CHCl_3$ and added into reaction solution to prevent residual thiol as an end group. After another 0.5 h, the solution was diluted with $CHCl_3$ (20 mL) and butylated hydroxytoluene (BHT) (0.11 g, 5.0×10^{-4} mol) was added to limit interchain crosslinking. The polymer solution was then precipitated into diethyl ether (300 mL) and collected by decanting the supernatant. The polymer was then dissolved in $CHCl_3$ (50 mL) and reprecipitated into diethyl ether (300 mL), collected by decanting the supernatant, and dried in vaccuo at room temperature for 24 h to obtain the pale-yellow polymer (3.43 g, 90 %). ^{1}H NMR ($CDCl_3$, 300 MHz): % *cis*: % *trans* = 82 %: 18 %, and *cis* content was determined by vinyl proton resonances in Figure S5.SEC (DMF + 0.1M LiBr, based on PS standards): M_n = 52.9 kDa, M_w = 94.4 kDa, $Đ_M$ = 1.8. DSC: T_g = 12 °C, T_c = 78 °C, T_m = 108 °C. TGA: T_d = 347 °C. Tensile tests: E_0 = 3.6 ± 0.1 MPa, ε_{break} = 1393 ± 11 %, UTS = 39.1 ± 0.7 MPa.

Synthesis of 71% cis content: The polymer was prepared by the general procedure described above by using DMSO/$CHCl_3$ (v/v: 1/3) co-solvent system with Et_3N as organic base. ^{1}H NMR ($CDCl_3$, 300 MHz): % *cis*: % *trans* = 71 %: 29 %, and *cis* content was determined by vinyl proton resonances in Figure S7. SEC (DMF + 0.1M LiBr,

based on PS standards): M_n = 51.3 kDa, M_w = 98.2 kDa, $Đ_M$ = 1.9. T_g = 9 °C. TGA: T_d = 341 °C. Tensile tests: E_0 = 2.1 ± 0.1 MPa, ε_{break} = 1656 ± 27 %, UTS = 38.1 ± 2.5 MPa.

Synthesis of 62% cis content: The polymer was prepared by the general procedure described above by using DMSO/$CHCl_3$ (v/v: 1/4) co-solvent system with Et_3N as organic base. ^{1}H NMR ($CDCl_3$, 300 MHz): % *cis*: % *trans* = 62 %: 38 %, and *cis* content was determined by vinyl proton resonances in Figure S9. SEC (DMF + 0.1M LiBr, based on PS standards): M_n = 56.0 kDa, M_w = 93.5 kDa, $Đ_M$ = 1.7. T_g = 3 °C. TGA: T_d = 346 °C. Tensile tests: E_0 = 1.7 ± 0.1 MPa, ε_{break} = 1669 ± 5 %, UTS = 26.0 ± 0.9 MPa.

Synthesis of 46% cis content: The polymer was prepared by the general procedure described above by using DMSO/$CHCl_3$ (v/v: 1/5) co-solvent system with Et_3N as organic base. ^{1}H NMR ($CDCl_3$, 300 MHz): % *cis*: % *trans* = 46 %: 54 %, and *cis* content was determined by vinyl proton resonances in Figure S11. SEC (DMF + 0.1M LiBr, based on PS standards): M_n = 45.8 kDa, M_w = 100.6 kDa, $Đ_M$ = 2.2. T_g = 1 °C. TGA: T_d = 315 °C. Tensile tests: E_0 = 5.0 ± 0.5 MPa, ε_{break} = 1056 ± 22 %, UTS = 5.4 ± 0.5 MPa.

Synthesis of 32% cis content: The polymer was prepared by the general procedure described above by using DMSO/$CHCl_3$ (v/v: 1/6) co-solvent system with Et_3N as organic base in Figure S13. ^{1}H NMR ($CDCl_3$, 300 MHz): % *cis*: % *trans* = 32 %: 68 %, and *cis* content was determined by vinyl proton resonances. SEC (DMF + 0.1M LiBr, based on PS standards): M_n = 34.5 kDa, M_w = 74.0 kDa, $Đ_M$ = 2.1. T_g = -1 °C. TGA: T_d = 320 °C. Tensile tests: E_0 = 4.0 ± 0.1 MPa, ε_{break} = 785 ± 66 %, UTS = 2.6 ± 0.2 MPa.

RESULTS AND DISCUSSION

Monomer and Polymer Syntheses

As depicted in Scheme 1, the synthesis of the urethane-based dipropiolate monomer, 5,14-dioxo-4,15-dioxa-6,13-diazaoctadecane-1,18-diyl dipropiolate (**U_6**), began from 3-bromo-1-propanol (**1**) reacted with hexamethylene diisocyanate (HDI) with catalytic dibutyltin dilaurate to afford the dibromo-substituted urethane compound, bis(3-bromopropyl) hexane-1,6-diyl dicarbamate (**2**). Further nucleophilic substitution (S_N2) of dibromo-substituted

urethane (**2**) was successfully accomplished by reacting with sodium propiolate to obtain the urethane-based dipropiolate monomer (**U_6**) (See Figure 1A).

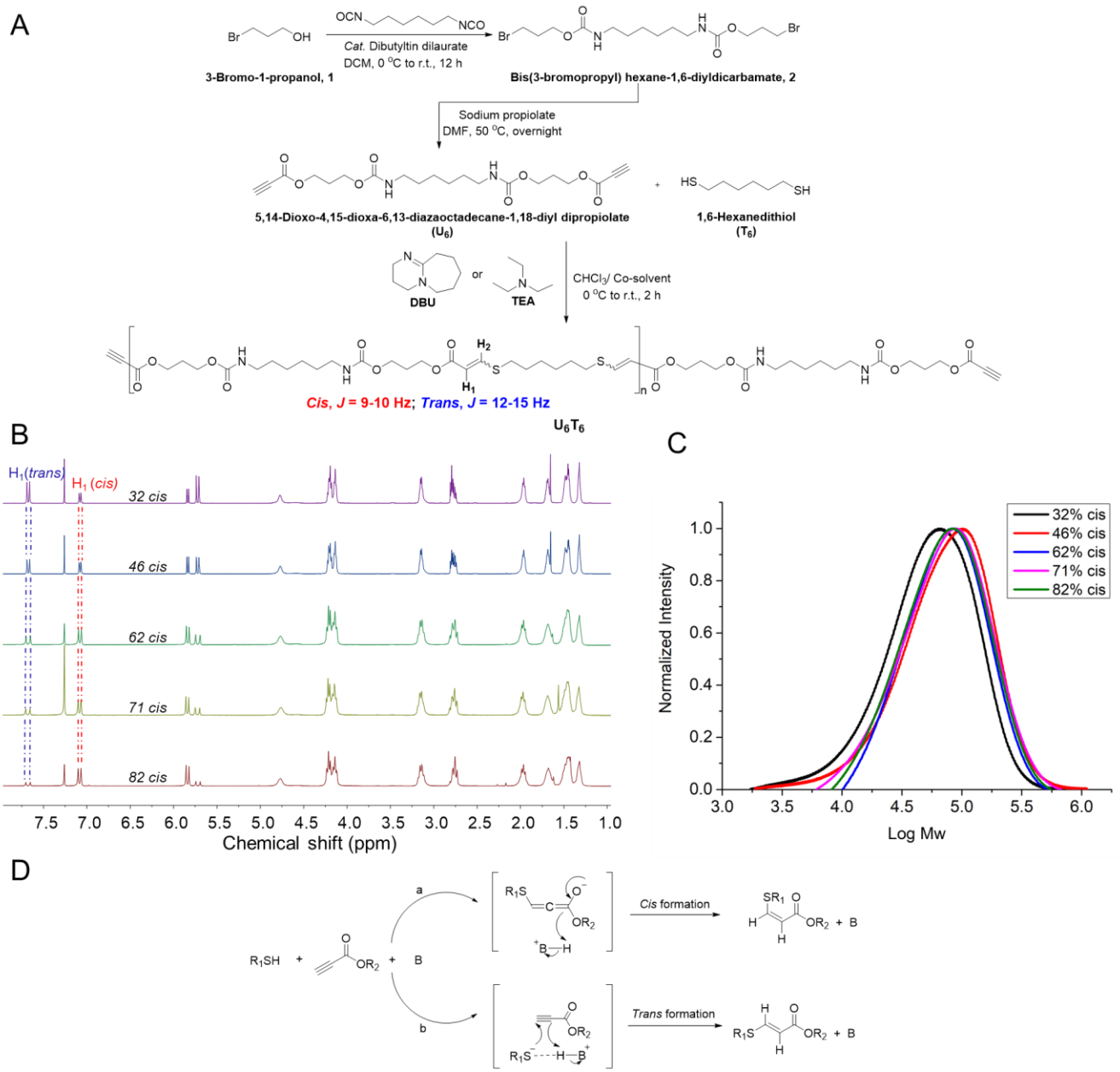

Figure 1. Characterization of stereocontrolled polyurethanes. **A)** A base-directed thiol-yne step-growth polymerization for different %*cis* content polymers was carried out with 5,14-dioxo-4,15-dioxa-6,13-diazaoctadecane-1,18-diyl dipropiolate (**U_6**) and the distilled 1,6-hexanedithiol (**T_6**) in different solvents and catalytic bases. **B)** Stacked ^{1}H NMR spectra in $CDCl_3$ demonstrated two clear vinyl proton doublets at δ = 7.1 ppm (*cis*, 9 Hz) and δ = 7.7 ppm (*trans*, 15 Hz), respectively. Significantly, the ratio of the *cis* to *trans* is determined by the resonance H_1 to reveal the stereochemistry can be controlled under thiol-yne step-growth polymerization with specific solvent and catalytic base. **C**) SEC chromatograms determined by polystyrene (PS) standards for

polyurethanes with tunable stereochemistry. **D)** Mechanisms of how to control the *cis* and *trans* configuration through the base and solvent modulation.[35]

The combination of 5,14-dioxo-4,15-dioxa-6,13-diazaoctadecane-1,18-diyl dipropiolate (**U_6**), the distilled 1,6-hexanedithiol (**T_6**), and 1.0 mol% 1,8-diazabicyclo[5.4.0]undec-7-ene (DBU) in chloroform yielded **U_6T_6** polymer with 82% *cis* content (M_n = 52.9 kDa, M_w = 94.4 kDa, $Đ_M$ = 1.8). (see Figure 1A and Table 1). Correspondingly, the %*cis* content can be identified by *J* coupling (J_{cis} = 9 Hz and J_{trans} = 15 Hz), and be quantitatively calculated by the integration of *cis* and *trans* vinyl protons H_1 using the ^{1}H NMR spectra shown in Figure 1B. Prototypical conditions (Et_3N as basic catalyst and DMF as co-solvent in chloroform) were utilized to achieve relatively low %*cis* content polymers.[28, 36, 39] Unfortunately, the polymer gradually precipitated out due to poor solubility. In order to achieve the targeted %*cis* content with high molar mass, we replaced DMF with DMSO as a co-solvent in $CHCl_3$ while maintaining Et_3N as the organic base catalyst. Four distinct volume ratios of DMSO (25%, 20%, 16.7%, and 14.3%) were used to provide various %*cis* content polymers with high molar mass. All polymerization conditions and molar masses are listed in **Table 1**.

Table 1. Stereochemistry and molecular masses of thiol-yne polymers (**U_6T_6**) were obtained using different polymerization conditions from 5,14-dioxo-4,15-dioxa-6,13-diazaoctadecane-1,18-diyl dipropiolate (**U_6**) and 1,6-hexanedithiol (**T_6**) precursors and thermal properties were obtained by DSC.

%*Cis*	Solvent	Base	M_n (kDa)	M_w (kDa)	$Đ_M$	T_g (°C)	T_d (°C)
82	$CHCl_3$	DBU	52.9	94.4	1.8	12	347
71	DMSO/$CHCl_3$ (1:3)	Et_3N	51.3	98.2	1.9	9	341
62	DMSO/$CHCl_3$ (1:4)	Et_3N	56.0	93.5	1.7	3	346
46	DMSO/$CHCl_3$ (1:5)	Et_3N	45.8	100.6	2.2	1	315
32	DMSO/$CHCl_3$ (1:6)	Et_3N	34.5	74.0	2.1	-1	320

Thermal and Mechanical Properties

The thermal properties of the materials were investigated by using differential scanning calorimetry (DSC) to observe the glass transition (T_g), crystalline (T_c), and melting (T_m) temperatures and by using thermogravimetric analysis (TGA) to characterize the degradation temperature (T_d). All three different %*cis* $\mathbf{U_6T_6}$ stereoelastomers exhibited glass transitions (T_g) while no melting nor crystalline temperatures were observed during the 2nd heating and 1st cooling cycle at 10 °C/min ramp speed. Moreover, the T_g trend shown in Figure 2A displayed a positive correlation with %*cis* content. 82% *cis* content stereoelastomer possessed the highest glass transition temperature (T_g = 12 °C) while 32% *cis* content analog had the lowest glass transition (T_g = -1 °C). The glass transition of 82% *cis* was then screened using three different ramp speeds (10 °C/min, 5 °C/min, and 1 °C/min) which showed the T_g gradually decreased from 12 °C to 7 °C (see Figure 2B). Interestingly, crystalline (T_c = 78 °C) and melting (T_m = 108 °C) temperatures were only detected for the 82% *cis* stereoelastomer during the heating cycle. The thermal-induced crystallinity of 82% *cis* at slow ramp speeds (1 °C/ min) revealed the highest %*cis* content which enables better hydrogen bonding interactions between urethane units on polymer backbones. These results suggested that all materials were predominantly amorphous.

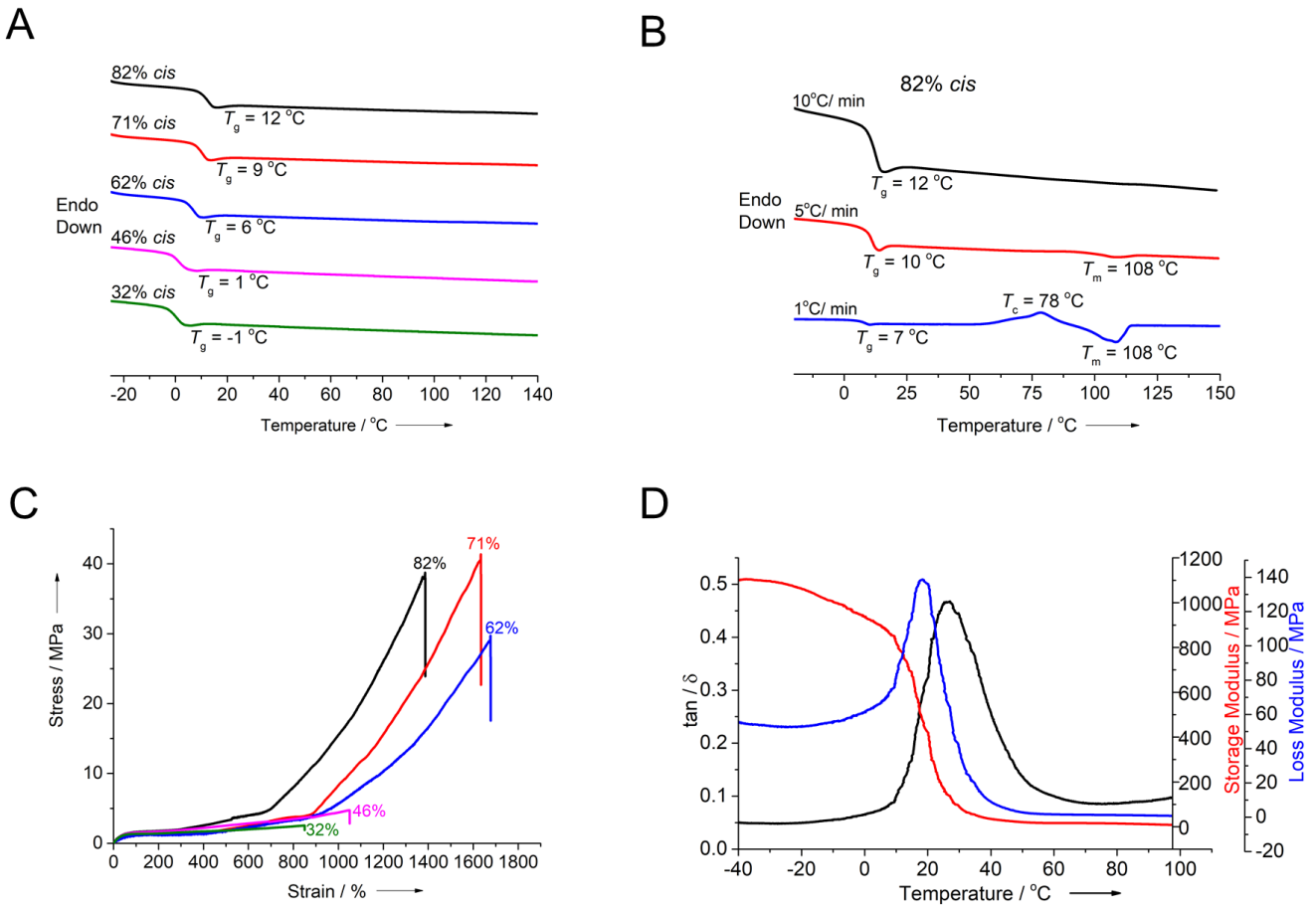

Figure 2. Thermomechanical characterization of polyurethane stereoelastomers. **A**) DSC thermograms of the 2nd heating cycle presented for $\mathbf{U_6T_6}$ with five different %*cis*. Higher *cis* content revealed higher glass transition temperature (T_g) to show more stiffer property. **B**) DSC thermograms of the 2nd heating cycle with three different ramp speeds presented for 82% *cis* content. Polymer chains formed better chain packing by hydrogen bonding interaction resulting in remarkable thermal-induced crystallinity (T_c) at 78 °C under slow ramp speed. **C**) Representative stress *vs.* strain curves for $\mathbf{U_6T_6}$ with the various %*cis* content at 10 mm/ min under room temprerature. **D**) Storage modulus, loss modulus, and tan δ were presented by a DMA temperature ramp-frequency sweep for the 82% *cis* content stereoelastomer.

Mechanical properties were investigated for $\mathbf{U_6T_6}$ with various stereochemistry are listed in Table 2. The Young's modulus, extension at break, and strain at break were all determined from the stress *vs.* strain curves obtained using tensile testing. The differences of Young's modulus (E) of all polymers are not distinctive. This is attributed to each of the species having a glass transition temperature (T_g) below room temperature while also being predominantly amorphous. The 82% *cis* content displayed significant strain-induced crystallization and strain-hardening after it was elongated over 600% of strain. Additionally, Fourier-transform infrared (FT-IR) spectroscopy

was used to study hydrogen bonding interactions. The stretches at 3334 cm^{-1} and 1686 cm^{-1} from the 82% *cis* stereoelastomer are associated with hydrogen bonding between amide N-H and C=O groups, respectively.[40] Thus, the results from FT-IR support the hypothesis of hydrogen bonding between urethane linkages (see Figure S16 for details). The 32% *cis* content exhibits the lowest strain at break (ε_{break}%) 785 ± 66 % (see Figure 3C) due to reduced hydrogen bonding effect resulting from twisting configuration of polymer backbones based on increase of %*trans* content. Notably, mechanical properties of 71% *cis* not only revealed exactly same UTS (39.1 ± 0.7) as 82% *cis* but also performed elongation at strain break (ε_{break}%) 1656 ± 27 % which is similar as 71% *cis*. Mechanical performance of 71% *cis* based on representative stress *vs* strain curves suggested that 71% *cis* stereochemistry would be enough to concomitantly obtain maximum UTS and elongation for the species under study once hydrogen bonding system incorporated.

Table 2. Thermal and mechanical properties for five different %*cis* $\mathbf{U_6T_6}$ polymers.

%*Cis*	E_0 (MPa)	ε_{beak} (%)	UTS (MPa)
82	3.6 ± 0.1	1393 ± 11	39.1 ± 0.7
71	2.1 ± 0.1	1656 ± 27	38.1 ± 2.5
62	1.7 ± 0.1	1669 ± 10	26.0 ± 0.9
46	5.0 ± 0.8	1056 ± 22	5.4 ± 0.5
32	4.0 ± 0.1	785 ± 66	2.6 ± 0.2

DMA Tests and Shape Memory Properties

The shape memory properties were tested by using a DMA Q800 instrument with cyclic thermomechanical testing over three cycles. Testing was completed in controlled force mode with heating and cooling rates of 10 °C/ min. As a proof of concept for shape memory based on hydrogen bonding, a 82% *cis* content stereoelastomer was chosen to perform thermomechanical behavior. After investigated by temperature sweep, a storage modulus drop was observed at the glass transition temperature (T_g), followed by a rubbery-like plateau (see red line in Figure 2D). This feature shows that the material has thermally stimulated shape memory properties. The large peak in loss modulus (see blue transition in Figure) revealed activation of molecular mobility and the rubbery-plateau indicated the presence of a network based on hydrogen bonding that is responsible for shape transformations.[41-43] The material (82% *cis*) was examined with three shape memory cycles (see Figure 3A). The depicted results show the 1st cycle shape recovery was ~24%. Nevertheless, the 2nd and 3rd cycle displayed significant shape recovery improvement

(~90%), and all of three cycles presented ideal fixity (~98.5%).

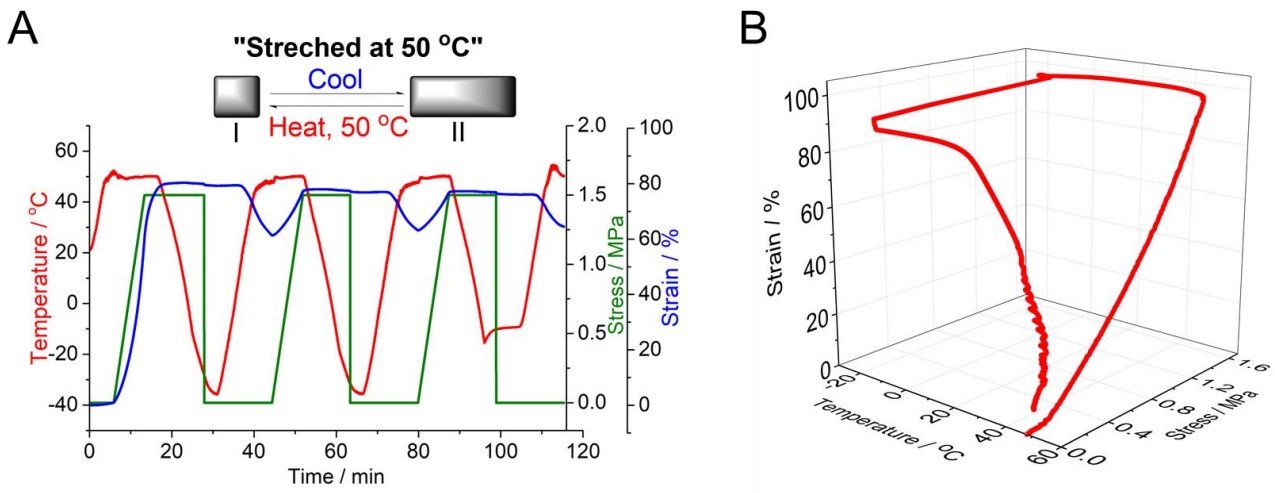

Figure 3. Shape Memory characterization of 82% *cis* content stereoelastomer. **A**) Representative curves of three shape memory cycles for 82% *cis* content stereoelastomer are shown. **B**) Visual demonstration of shape memory is observed in the 3rd cycle for the 82% *cis* content stereoelastomer by heating to 50 °C and the shape is shown to recover up to 90%.

Unlike most shape memory materials based on covalently crosslinked bonding system,[44, 45] the properties of the polyurethane stereoelastomers are based on hydrogen bonding within the urethane units which function as physical crosslinking units.[40, 46, 47] When the material is heated, the hydrogen bonding orientation is disordered. However, the DSC thermogram of the 82% *cis* content showed a thermally induced crystalline transition (T_c) indicating that when the material was heated close to the onset of T_c, additional highly ordered hydrogen bonds would be formed. The result of thermomechanical analysis from the 1st cycle matched the observation from DSC as well. Significantly, part of the polymer chains with weaker or disordered hydrogen bonding interaction exist in an amorphous domain which plays a key role in the shape recovery from the 2nd cycle that improve shape recovery performance from 24% to 90%. These features make urethane-based elastomer distinct from other SMP systems that depend on crosslinked chemical bonds, copolymers, polymers with blending, and classic physical crosslinking bond (H-bond) to form the network. In Figure 3B, a visual demonstration with a three-dimensional plot of the 3rd cycle for 82% *cis* content is shown as it performs an ideal shape recovery process.

Accelerated Degradation and Biocompatibility Studies

The hydrolytic stability was assessed for all three different %*cis* $\mathbf{U_6T_6}$ polymers and molar masses were listed in Table 1. All testing samples for degradation studies were prepared by compression molding of a film with 0.5 mm thickness, cut into discs with 4 mm in diameter, and tested using accelerated degradation conditions in 5 M NaOH solution at 37 °C + 5% CO_2 for up to 12 weeks. The results show that degradation rates are highly dependent on the %*cis* conformation of α,β-unsaturated alkenes on the backbone (see Figure 4A and 4B). The lower %*cis* content provides more flexibility to increase the chain mobility matched the DSC thermograms (see Figure 2A) and helps to accelerates the degradation rate through increased water penetration into the discs. SEM analysis of tested coupons from the accelerated degradation conditions on the 62% *cis* polymer indicates uniform degradation and confirms surface erosion as the predominant degradation process (see Figure 4C).[48]

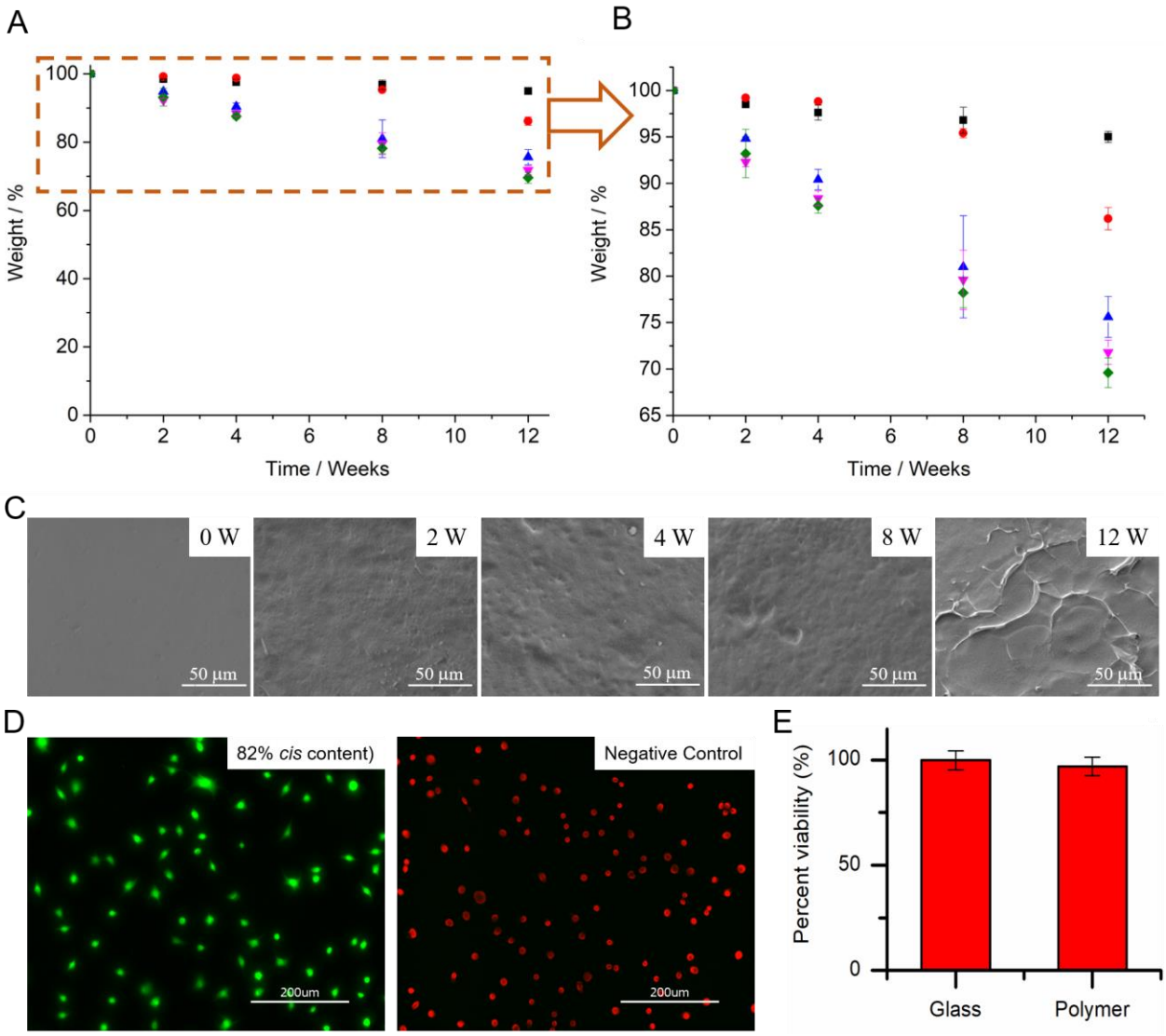

Figure 4. A) Mass loss over time with different %*cis* elastomers (black: 82%; red: 71%; blue: 62%; pink: 46%; olive: 32%, respectively) shows stereochemistry dependent surface erosion behavior. **B**) Enlarged scale at degradation region. **C**) SEM analysis of test coupons from 62% *cis* content exposed to accelerated degradation conditions indicates uniform degradation from surface erosion processes. Cell viability of 82% *cis* content. **D**) LIVE/DEAD imaging at 20× magnification of L929 cells on a 82% cis stereoelastomer disc and after exposure to 70% EtOH for 1 h. **E**) Cell viability as measured by XTT assay.

To assess further potential cytotoxicity from these materials, stereoelastomer samples with 82% *cis* content were seeded with L929 fibroblasts and cell viability was evaluated for 48 h after cell seeding. LIVE/DEAD imaging showed that cells viability was nearly quantitative as assessed by XTT assay and nearly identical to L929's seeded on glass slides (Figures 3D and 3E). These data suggest that the urethane-based elastomers are compatible with

cells and have potential use as an implantable biomaterial.

CONCLUSION

The urethane-based dipropiolate, 5,14-dioxo-4,15-dioxa-6,13-diazaoctadecane-1,18-diyl dipropiolate, was successfully synthesized and utilized as a new class of dipropiolic monomer that can further be polymerized using stereo-chemically controlled thiol-yne Michael additions to yield polyurethanes. The thermal and mechanical properties are tunable by varying the stereochemistry of the alkene unit from 82% to 32% *cis* content in the polymer backbone. Amorphous polymers possessing hydrogen bonding along the backbone retain their mechanical properties. The thermomechanical analysis of 82% *cis* content polymer displayed shape memory behavior. The investigation of accelerated degradation behavior in 5 M NaOH solution up to a three-month period has displayed the materials with reduced %*cis* content yielded faster degradation rates thus demonstrating that stability of material is highly stereo-chemically dependent. *In vitro* cell viability of 82% *cis* content has indicated urethane-based elastomers possess excellent biocompatibility. The combination of biocompatible, biostable, and tunable thermal and mechanical properties supports our material as potentially new candidates for a long-term implantable biomaterial and biomedical device. Nonetheless, biodegradable polymeric materials might be more valuable for soft tissue engineering due to degraded segments would be expected to be non-toxic and resorbable in biological systems. Importantly, a well-known degradable unit such as an ester moiety can be easily incorporated into our polyurethane backbone and formulated as copolymer systems could provide a series of resorbable polymers in the future.

ASSOCIATED CONTENT

Supporting Information (SI). Synthetic schemes and details, ^{1}H NMR and ^{13}C NMR spectra, polymer characterization, mechanical property measurements, cell viability measurements.

AUTHOR INFORMATION

Corresponding Authors

*Matthew L. Becker, email: matthew.l.becker@duke.edu

*Andrew P. Dove, email: a.dove@bham.ac.uk

Author Contributions

A.P.D. and M.L.B. conceived the project idea. Y-H.H. and M.L.B. designed the materials and synthetic routes while Y-H.H. synthesized and characterized the materials. Y-H.H. performed thermal, mechanical analyses and *in vitro* degradation studies and performed DMA analyses. Y-H.H. and D.L. prepared *in vitro* cell Live/Dead samples while D.L. performed and analyzed cell viability. Y-H.H. prepared the samples of SEM analysis while D.A. performed and analyzed SEM images. Y-H.H., A.P.D., and M.L.B. wrote the manuscript, all authors edited and commented on the manuscript.

ACKNOWLEDGMENT

The authors gratefully acknowledge Duke University for financial support. Mass spectrometry was performed by Benqian Wei in the lab of Dr. Chrys Wesdemiotis at The University of Akron Mass Spectrometry Center. The authors also acknowledge Samantha McDonald and Dr. Metin Karayilan with characterization assistance during the revision process.

REFERENCES

1. Engels, H. W.; Pirkl, H. G.; Albers, R.; Albach, R. W.; Krause, J.; Hoffmann, A.; Casselmann, H.; Dormish, J., Polyurethanes: Versatile Materials and Sustainable Problem Solvers for Today's Challenges. *Angew. Chem. Int. Ed.* **2013,** *52* (36), 9422-9441.

2. Golling, F. E.; Pires, R.; Hecking, A.; Weikard, J.; Richter, F.; Danielmeier, K.; Dijkstra, D., Polyurethanes for coatings and adhesives - chemistry and applications. *Polym. Int.* **2019,** *68* (5), 848-855.

3. Gama, N.; Ferreira, A.; Barros-Timmons, A., 3D printed cork/ polyurethane composite foams. *Mater. Design* **2019,** *179*, 107905-107913.

4. Knaub, P. M. A.; Wiltz, E. P.; Wuilay, H., A new era for MDI: Flexible polyurethane slabstock foam. *J. Cell. Plast.* **1997,** *33* (2), 159-184.

5. Singh, S. N.; Lynch, J. J.; Daems, D., Techniques to assess the various factors affecting the long term dimensional stability of rigid polyurethane foam. *J. Cell Plast.* **1996,** *32* (6), 553-578.

6. Overbeek, A., Polymer heterogeneity in waterborne coatings. *J. Coat. Technol. Res.* **2010,** *7* (1), 1-21.

7. Yang, X. F.; Vang, C.; Tallman, D. E.; Bierwagen, G. P.; Croll, S. G.; Rohlik, S., Weathering degradation of a polyurethane coating. *Polym. Degrad. Stabil.* **2001,** *74* (2), 341-351.

8. Du, H.; Zhao, Y. H.; Li, Q. F.; Wang, J. W.; Kang, M. Q.; Wang, X. K.; Xiang, H. W., Synthesis and characterization of waterborne polyurethane adhesive from MDI and HDI. *J. Appl. Polym. Sci.* **2008,** *110* (3), 1396-1402.

9. Gogolewski, S., Selected Topics in Biomedical Polyurethanes - a Review. *Colloid Polym Sci* **1989,** *267* (9), 757-785.

10. Chatterjee, S.; Saxena, M.; Padmanabhan, D.; Jayachandra, M.; Pandya, H. J., Futuristic medical implants

using bioresorbable materials and devices. *Biosens. Bioelectron.* **2019,** *142,* 111489-111500.

11. Son, J. S.; Lee, S. H.; Lee, B.; Kim, H. J.; Ko, J. H.; Park, Y. H.; Chun, H. J.; Kim, C. H.; Kim, J. H.; Kim, M. S., Polyurethanes for Biomedical Application. *Tissue Eng. Regen. Med.* **2009,** *6* (4-11), 427-431.

12. Zander, Z. K.; Chen, P. R.; Hsu, Y. H.; Dreger, N. Z.; Savariau, L.; Mcroy, W. C.; Cerchiari, A. E.; Chambers, S. D.; Barton, H. A.; Becker, M. L., Post-fabrication QAC-functionalized thermoplastic polyurethane for contact-killing catheter applications. *Biomaterials* **2018,** *178*, 339-350.

13. Lendlein, A.; Langer, R., Biodegradable, elastic shape-memory polymers for potential biomedical applications. *Science* **2002,** *296* (5573), 1673-1676.

14. Shimada, R.; Konishi, H.; Ozawa, H.; Katsumata, T.; Tanaka, R.; Nakazawa, Y.; Nemoto, S., Development of a new surgical sheet containing both silk fibroin and thermoplastic polyurethane for cardiovascular surgery. *Surg. Today* **2018,** *48* (5), 486-494.

15. Klement, P.; Du, Y. J.; Berry, L. R.; Tressel, P.; Chan, A. K. C., Chronic performance of polyurethane catheters covalently coated with ATH complex: A rabbit jugular vein model. *Biomaterials* **2006,** *27* (29), 5107-5117.

16. Nowatzki, P. J.; Koepsel, R. R.; Stoodley, P.; Min, K.; Harper, A.; Murata, H.; Donfack, J.; Hortelano, E. R.; Ehrlich, G. D.; Russell, A. J., Salicylic acid-releasing polyurethane acrylate polymers as anti-biofilm urological catheter coatings. *Acta Biomater.* **2012,** *8* (5), 1869-1880.

17. Grover, N.; Plaks, J. G.; Summers, S. R.; Chado, G. R.; Schurr, M. J.; Kaar, J. L., Acylase-containing polyurethane coatings with anti-biofilm activity. *Biotechnol. Bioeng.* **2016,** *113* (12), 2535-2543.

18. Khil, M. S.; Cha, D. I.; Kim, H. Y.; Kim, I. S.; Bhattarai, N., Electrospun nanofibrous polyurethane membrane as wound dressing. *J. Biomed. Mater. Res. B* **2003,** *67b* (2), 675-679.

19. Ozkaynak, M. U.; Atalay-Oral, C.; Tantekin-Ersolmaz, S. B.; Guner, F. S., Polyurethane films for wound dressing applications. *Macromol. Symp.* **2005,** *228*, 177-184.

20. Gultekin, G.; Atalay-Oral, C.; Erkal, S.; Sahin, F.; Karastova, D.; Tantekin-Ersolmaz, S. B.; Guner, F. S., Fatty acid-based polyurethane films for wound dressing applications. *J. Mater. Sci.-Mater. M.* **2009,** *20* (1), 421-431.

21. Chien, Y. C.; Chuang, W. T.; Jeng, U. S.; Hsu, S. H., Preparation, Characterization, and Mechanism for Biodegradable and Biocompatible Polyurethane Shape Memory Elastomers. *ACS Appl. Mater. Inter.* **2017,** *9* (6), 5419-5429.

22. Stubbs, C. J.; Worch, J. C.; Prydderch, H.; Becker, M. L.; Dove, A. P., Unsaturated Poly(ester-urethanes) with Stereochemically Dependent Thermomechanical Properties. *Macromolecules* **2020,** *53* (1), 174-181.

23. Cho, J. W.; Kim, J. W.; Jung, Y. C.; Goo, N. S., Electroactive shape-memory polyurethane composites incorporating carbon nanotubes. *Macromol. Rapid. Comm.* **2005,** *26* (5), 412-416.

24. Lendlein, A.; Jiang, H. Y.; Junger, O.; Langer, R., Light-induced shape-memory polymers. *Nature* **2005,** *434* (7035), 879-882.

25. Lendlein, A.; Schmidt, A. M.; Langer, R., AB-polymer networks based on oligo(epsilon-caprolactone) segments showing shape-memory properties. *P. Natl. Acad. Sci. USA* **2001,** *98* (3), 842-847.

26. Chen, H. M.; Li, Y.; Liu, Y.; Gong, T.; Wang, L.; Zhou, S. B., Highly pH-sensitive polyurethane exhibiting

shape memory and drug release. *Polym. Chem.* **2014,** *5* (17), 5168-5174.

27. Wei, H. Q.; Zhang, Q. W.; Yao, Y. T.; Liu, L. W.; Liu, Y. J.; Leng, J. S., Direct-Write Fabrication of 4D Active Shape-Changing Structures Based on a Shape Memory Polymer and Its Nanocomposite. *ACS Appl. Mater. Inter.* **2017,** *9* (1), 876-883.

28. Worch, J. C.; Weems, A. C.; Yu, J.; Arno, M. C.; Wilks, T. R.; Huckstepp, R. T. R.; O'Reilly, R. K.; Becker, M. L.; Dove, A. P., Elastomeric polyamide biomaterials with stereochemically tuneable mechanical properties and shape memory. *Nat. Commun.* **2020,** *11* (1), 3250.

29. Santerre, J. P.; Woodhouse, K.; Laroche, G.; Labow, R. S., Understanding the biodegradation of polyurethanes: From classical implants to tissue engineering materials. *Biomaterials* **2005,** *26* (35), 7457-7470.

30. Liu, Q. Y.; Jiang, L.; Shi, R.; Zhang, L. Q., Synthesis, preparation, in vitro degradation, and application of novel degradable bioelastomers-A review. *Prog. Polym. Sci.* **2012,** *37* (5), 715-765.

31. Goodman, A.; Schilder, H.; Aldrich, W., Thermomechanical Properties of Gutta-Percha .2. History and Molecular Chemistry of Gutta-Percha. *Oral. Surg. Oral. Med. O.* **1974,** *37* (6), 954-961.

32. Yao, K. C.; Nie, H. R.; Liang, Y. R.; Qiu, D.; He, A. H., Polymorphic crystallization behaviors in cis-1,4-polyisoprene/trans-1,4-polyisoprene blends. *Polymer* **2015,** *80*, 259-264.

33. Worch, J. C.; Prydderch, H.; Jimaja, S.; Bexis, P.; Becker, M. L.; Dove, A. P., Stereochemical enhancement of polymer properties. *Nat. Rev. Chem.* **2019,** *3* (9), 514-535.

34. Jim, C. K. W.; Qin, A.; Lam, J. W. Y.; Mahtab, F.; Yu, Y.; Tang, B. Z., Metal-Free Alkyne Polyhydrothiolation: Synthesis of Functional Poly(vinylenesulfide)s with High Stereoregularity by Regioselective Thioclick Polymerization. *Adv. Funct, Mater,* **2010,** *20* (8), 1319-1328.

35. Truong, V. X.; Dove, A. P., Organocatalytic, Regioselective Nucleophilic "Click" Addition of Thiols to Propiolic Acid Esters for Polymer-Polymer Coupling. *Angew. Chem. Int. Ed.* **2013,** *52* (15), 4132-4136.

36. Bell, C. A.; Yu, J. Y.; Barker, I. A.; Truong, V. X.; Cao, Z.; Dobrinyin, A. V.; Becker, M. L.; Dove, A. P., Independent Control of Elastomer Properties through Stereocontrolled Synthesis. *Angew. Chem. Int. Ed.* **2016,** *55* (42), 13076-13080.

37. Zhao, Q.; Qi, H. J.; Xie, T., Recent progress in shape memory polymer: New behavior, enabling materials, and mechanistic understanding. *Prog. Polym. Sci.* **2015,** *49-50*, 79-120.

38. Yang, J.; Hong, K. L.; Bonnesen, P. V., A method for preparing sodium acrylate-d(3), a useful and stable precursor for deuterated acrylic monomers. *J. Label. Compd. Rad.* **2011,** *54* (12), 743-748.

39. Hsu, Y. H.; Dove, A. P.; Becker, M. L., Crosslinked Internal Alkyne-Based Stereo Elastomers: Polymers with Tunable Mechanical Properties. *Macromolecules* **2021,** *54*, 10, 4649–4657.

40. Coleman, M. M.; Skrovanek, D. J.; Hu, J. B.; Painter, P. C., Hydrogen-Bonding in Polymer Blends .1. Ftir Studies of Urethane Ether Blends. *Macromolecules* **1988,** *21* (1), 59-65.

41. Xie, T., Recent advances in polymer shape memory. *Polymer* **2011,** *52* (22), 4985-5000.

42. Peterson, G. I.; Dobrynin, A. V.; Becker, M. L., alpha-Amino Acid-Based Poly(Ester urea)s as Multishape Memory Polymers for Biomedical Applications. *ACS Macro. Lett.* **2016,** *5* (10), 1176-1179.

43. Peterson, G. I.; Childers, E. P.; Li, H.; Dobrynin, A. V.; Becker, M. L., Tunable Shape Memory Polymers from alpha-Amino Acid-Based Poly(ester urea)s. *Macromolecules* **2017,** *50* (11), 4300-4308.
44. Le, D. M.; Kulangara, K.; Adler, A. F.; Leong, K. W.; Ashby, V. S., Dynamic Topographical Control of Mesenchymal Stem Cells by Culture on Responsive Poly(epsilon-caprolactone) Surfaces. *Adv. Mater.* **2011,** *23* (29), 3278.
45. Neuss, S.; Blomenkamp, I.; Stainforth, R.; Boltersdorf, D.; Jansen, M.; Butz, N.; Perez-Bouza, A.; Knuchel, R., The use of a shape-memory poly(epsilon-caprolactone)dimethacrylate network as a tissue engineering scaffold. *Biomaterials* **2009,** *30* (9), 1697-705.
46. Luo, N.; Wang, D. N.; Ying, S. K., Hydrogen-bonding properties of segmented polyether poly(urethane urea) copolymer. *Macromolecules* **1997,** *30* (15), 4405-4409.
47. Teo, L. S.; Chen, C. Y.; Kuo, J. F., Fourier transform infrared spectroscopy study on effects of temperature on hydrogen bonding in amine-containing polyurethanes and poly(urethane-urea)s. *Macromolecules* **1997,** *30* (6), 1793-1799.
48. Wandel, M. B.; Bell, C. A.; Yu, J.; Arno, M. C.; Dreger, N. Z.; Hsu, Y. H.; Pitto-Barry, A.; Worch, J. C.; Dove, A. P.; Becker, M. L., Concomitant control of mechanical properties and degradation in resorbable elastomer-like materials using stereochemistry and stoichiometry for soft tissue engineering. *Nat. Commun.* **2021,** *12* (1), 446.

TOC